THE JOURNAL OF PHYSICAL CHEMISTRY C

Article

Cite This: J. Phys. Chem. C 2019, 123, 28100−28105

pubs.acs.org/JPCC

Dynamics of Short-Lived Polaron Pairs and Polarons in Polythiophene Derivatives Observed via Infrared-Activated Vibrations

Klara Stallhofer,[†] Matthias Nuber,[†] Reinhard Kienberger,[†] Volker Körstgens,[‡] Peter Müller-Buschbaum,[‡,§] and Hristo Iglev*[,†]

[†]Physik-Department, Lehrstuhl für Laser- und Röntgenphysik and [‡]Physik-Department, Lehrstuhl für Funktionelle Materialien, Technische Universität München, James-Franck-Strasse 1, 85748 Garching, Germany

[§]Heinz Maier-Leibnitz Zentrum (MLZ), Technische Universität München, Lichtenbergstr. 1, 85748 Garching, Germany

Supporting Information

ABSTRACT: Infrared-activated vibrations in the fingerprint region induced by structural rearrangement of the polymer in the presence of a charge are used to identify polaronic species in femtosecond spectroscopy. This is possible without resorting to complex spectral modeling or excitation density dependence of the different charge carriers. Their dynamics are investigated in bulk heterojunctions formed of a polythiophene derivative with TiO_2 nanoparticle acceptors, as well as in the pure polymer. The water-soluble polymer poly[3-(potassium-6-hexanoate)thiophene-2,5-diyl] (P3P6T) is compared with the intensely studied poly(3-hexylthiophene-2,5-diyl) (P3HT). Distinct bands are attributed to polarons and polaron pairs. Pairs with a lifetime of a few picoseconds are generated within the time resolution. In the presence of the acceptor, polaron yield rises with respect to the generated polaron pairs. Diffusion of polarons from 10 ps onward is identified as being either of predominantly intrachain or interchain character, depending on the degree of order present in the polymer.

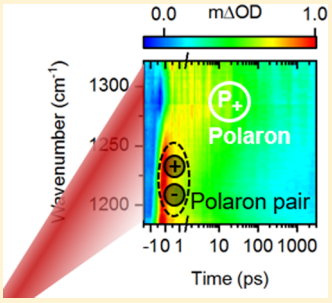

INTRODUCTION

For organic and hybrid solar cells built of a conjugated semiconducting polymer mixed with an appropriate acceptor, a plethora of bound and free charges has been stated and assigned to charge dynamics observed in time-resolved measurements. Prominent among these are excitons, polarons, and polaron pairs.[1,2]

Excitons, which are neutral electron−hole pairs bound by Coulombic attraction, are unanimously considered as primary photoexcitations. In the simplest picture, excitons dissociate to form free charges in the form of polarons. Polarons are quasiparticles formed by structural reorientation around a charge on the polymer backbone. In the conventional picture, this rearrangement leads to polaronic states that form two electronic levels offset from HOMO and LUMO within the band gap.[3] In the presence of an acceptor featuring a favorable band alignment with respect to the polymer, charge separation becomes much more efficient. Polaron pairs are neutral electron−hole pairs weakly bound via Coulomb interaction where the charges are each coupled to their own lattice distortion. They have been observed in time-resolved experiments covering the visible and infrared spectral regions, as well as in Raman studies investigating the C=C and C−C stretching regions.[4−6]

A clear distinction between different charged species in spectroscopic studies, which is the prerequisite for studying their respective dynamics, is not straightforward. It commonly relies on differing dependencies on excitation fluence.[7] Thus, regimes are often entered where additional processes, such as bimolecular recombination, dominate the picture.[8] Here, we show that different polaronic species can be clearly distinguished by observing the femtosecond to picosecond dynamics of respective charge-induced vibrational modes without the need for complex spectral decomposition. Besides the transitions from the in-gap polaronic levels, charges on the backbone of a polymer give rise to "infrared-activated vibrations" (IRAVs). In the presence of charges, these appear in the IR "fingerprinting" region and can serve as a quantitative measure of them in time-resolved experiments.[9] Interpreted within the framework of the "amplitude mode" model, IRAVs are derived from Raman modes of the neutral polymer. They become IR-active as a consequence of a local structural rearrangement of the polymer around the added charge that leads to a change in symmetry.[10] However, intense vibrational modes not directly linked to Raman modes, thus lying outside the scope of the amplitude model, have been observed and connected with the displacement of charge density by specific vibrations.[11] They are expected to be extremely sensitive to delocalization of the polaron.[12] Likewise, the enhanced vibrational modes are expected to be sensitive to the specific nature of the charge on the polymer and allow for distinguishing polaron and polaron pair dynamics.

Received: October 19, 2019
Published: October 25, 2019

DOI: 10.1021/acs.jpcc.9b09820
J. Phys. Chem. C 2019, 123, 28100−28105

We investigate the widely studied poly(3-hexylthiophene-2,5-diyl) (P3HT) since an extensive body of work on charge dynamics, covering a broad spectral and temporal range, exists for this polymer, as detailed below. Thus, P3HT serves as a reference to relate our findings to previous studies. As a variant, we include poly[3-(potassium-6-hexanoate)thiophene-2,5-diyl] (P3P6T). It shares the backbone with P3HT but differs in its side groups, which are water-soluble. As such, P3P6T offers potential for green technologies where the organic solvent can be avoided in the production process of photovoltaic devices.[13,14] In P3P6T, polaronic signatures including IRAVs are readily observable, even without time resolution, due to their extremely long-lived nature. Both polymers are combined with TiO_2 as an acceptor material. In the field of hybrid photovoltaics, this combination has been employed in various nanostructures.[15−19]

EXPERIMENTAL METHODS

Sample Preparation. Films were spray-deposited on substrates of CaF_2 (Korth Kristalle GmbH, 2 mm thickness) utilizing an airbrush system Grafo Typ 3 (Harder & Steenbeck). The pressure of the carrier gas nitrogen was set to 2 bar, and the distance between the sample and nozzle of the spray setup was kept at 16 cm. Poly(3-hexylthiophene-2,5-diyl) (P3HT) (M_W = 50−70 kDa, regioregularity 91−94%, Rieke Metals) was sprayed out of 10 mg/mL chlorobenzene solution. A layer of TiO_2 nanoparticles (P25, Evonik) was deposited from aqueous dispersion. A composite film of P3HT:TiO_2 was prepared by successively spray-depositing TiO_2 nanoparticles out of aqueous dispersion and P3HT from a chlorobenzene solution. Poly[3-(potassium-6-hexanoate)-thiophene-2,5-diyl] (P3P6T) (M_W = 55−65 kDa, regioregularity 82−90%, Rieke Metals) was sprayed out of a 10 mg/mL aqueous solution. The polymer was also used to deposit a composite film P3P6T:TiO_2 (2:1 (w/w)) with P25 TiO_2 nanoparticles. All films containing P3HT and P3P6T were thermally annealed for 10 min at 120 °C under nitrogen flow.

X-ray Diffraction. X-ray diffraction (XRD) measurements were performed using a conventional XRD instrument (Bruker D8 Advance, Karlsruhe, Germany) with a scintillation counter. A copper anode X-ray source of λ = 1.54 Å at 40 kV and 40 mA was operated. Crystallite sizes were calculated with the Scherrer equation using a Scherrer constant K = 0.94.

UV−vis and FTIR Absorption Spectroscopy. Steady-state UV−vis absorption spectra were recorded on a PerkinElmer Lambda 650s UV−vis spectrometer. The spectra presented in Figure 1c were corrected for scattering effects by extrapolating the scattering signal between 720 and 830 nm to the entire measurement range using a Rayleigh scattering approach.

Steady-state IR absorbance spectra were recorded with a Bruker Tensor 27 FTIR spectrometer. The photoinduced absorption (PIA) spectrum of P3P6T was measured with a Bruker IFS 66v/s FTIR spectrometer. Both FTIR spectrometers were purged with dry air.

Femtosecond Spectroscopy. To observe the spectral evolution and temporal dynamics of photoexcited species on ultrashort timescales, a pump-probe setup based on a Ti:sapphire amplifier (Libra, Coherent Inc., 130 fs, 800 nm, 1 kHz) was employed. Pump pulses at 500 nm were generated in a two-stage noncollinear optical parametric amplifier pumped with the second harmonic of the Ti:sapphire laser that fed the whole setup. Probe light was converted to the mid-infrared with the help of a two-stage optical parametric amplifier followed by difference-frequency mixing in a $AgGaS_2$ crystal. The probe was tuned to 1250 cm^{-1} (covering ∼200 cm^{-1}). The probe beam was split into two to provide an unpumped reference to determine the change in optical density upon excitation ($\Delta OD = -\log_{10}(T/T_0)$), where T is transmission measured through the excited sample and T_0 is the reference value without a pump pulse preceding the probe. Additionally, a chopper served the same purpose. Pump and probe beams were focused onto the sample, and the latter was detected on a 2 × 64 pixel HgCdTe detector after passing a spectrometer, resulting in a spectral resolution of about 2 cm^{-1}. Polarization of the pump-beam with respect to the probe and its energy was adjusted with a combination of $\lambda/2$ waveplate and broadband wire-grid polarizer. If not noted otherwise, the pump and probe first passed the 2 mm CaF_2 substrate before reaching the sample. Care was taken to limit the excitation density to some tens of $\mu J/cm^2$. The pump beam diameter was determined with the help of a beam camera to ∼150 μm. The data shown in Figures 2 and 3, as well as in Figure S2, were measured with a pump pulse energy of 10 nJ corresponding to an excitation fluence of about 50 $\mu J/cm^2$. The resulting low density of primary photoexcitations kept contributions from additional decay channels due to bimolecular recombination to

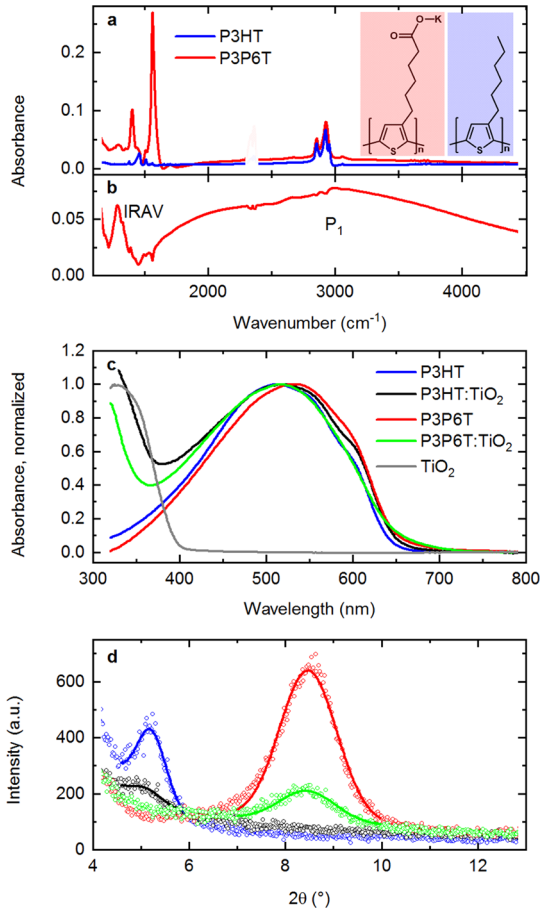

Figure 1. (a) IR absorption spectra of pure P3P6T and P3HT with the respective structures presented in the inset. (b) Photoinduced absorption of P3P6T showing a broad polaron absorption P_1 and IRAV mode. (c) UV−vis absorption of neat P3HT film, P3HT:TiO_2 layer-on-layer sample, neat P3P6T, P3P6T:TiO_2 composite, and a thin film of TiO_2 nanoparticles. (d) X-ray diffraction of the films with fits to the polymer peaks to determine crystallite sizes.

DOI: 10.1021/acs.jpcc.9b09820
J. Phys. Chem. C 2019, 123, 28100−28105

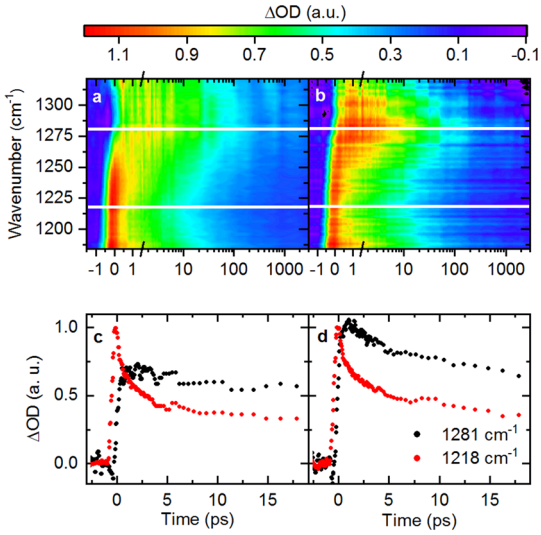

Figure 2. Pump-probe measurements of IRAV dynamics on P3P6T (left column) and P3P6T:TiO_2 (right column). Transients at spectral positions marked by horizontal white lines in the 2D plots (a,b) in the regions of polaron pair (1218 cm^{-1}) and polaron absorption (1281 cm^{-1}) are shown in panels (c) and (d).

a minimum. Subsequent measurements at the same sample position showed no change in amplitude or decay dynamics for P3HT and P3HT:TiO_2, demonstrating that the polymer samples are stable under the chosen excitation conditions. Due to the long-lived excitations in P3P6T that were observable in the FTIR measurements, there was a change for the pure P3P6T sample (see Figure S7). To minimize the influence, only the first scan was evaluated. Nonetheless, the observed changes in dynamics under prolonged excitation indicate that the lifetimes of photoexcited species are likely to be overestimated. No changes were observed in P3P6T:TiO_2 over the course of the measurement.

RESULTS AND DISCUSSION

Conventional and photoinduced-absorption (PIA) spectra that indicate the absorbance difference between the illuminated and dark samples of P3HT in the IR have been thoroughly investigated. Accordingly, distinct absorption peaks can be attributed to stretching vibrations of the alkyl chain between 2800 and 3090 cm^{-1} and respective bending modes as well as C=C stretching from 1400 to 1590 cm^{-1} in the FTIR spectra of neat P3HT presented in Figure 1a.[20] The side chain of P3P6T with its water-soluble end group adds an absorption at around 1290 cm^{-1} due to the C=O stretch, as well as two exceptionally intense carboxylate absorptions at 1402 and 1562 cm^{-1}.[21,22] PIA spectra feature a broad absorption attributable to polarons on the polymer chain, ranging from 2000 to 5500 cm^{-1}. Below 1500 cm^{-1}, the spectra are characterized by a collection of IRAVs.[23−26]

For P3P6T, strong spectral signatures are observable in both samples exposed to ambient light and in samples purposely illuminated. A broad polaron absorption band extending from 1750 to 5500 cm^{-1} is accompanied by an almost equally intense absorption around 1285 cm^{-1} (see Figure 1b). Absorption at the position of the two carboxylate stretch modes around 1500 cm^{-1} does not change upon illumination. The photoinduced spectral signatures decay over an extremely long period of several weeks. We emphasize that this effect is not due to degradation of the sample, as it is fully reversible (see Figure S1 in the Supporting Information). Complex formation with water has been shown to occur in conjugated polymer films and was suggested to result in similarly long-lived effects.[27] However, it seems unlikely here since formation of additional bonds is expected to alter the spectral shape in the IR region, not only the amplitude. We attribute the long-lived signatures to trapped polarons. To explore the trapping mechanism in detail lies beyond the scope of the present work. Processes involving light-induced structural changes in the polymer backbone[28] or trapping at morphological boundaries between aggregated and amorphous domains have been suggested.[29−32] Recently, polarons that are stable over months have been reported to occur in P3HT solution precursors.[33]

Ultraviolet−visible (UV−vis) spectra, which have been subtracted by a scattering contribution,[34] and X-ray diffraction (XRD) measurements show the more pronounced crystallinity of the P3HT samples, as compared to P3P6T samples. In the UV−vis spectra shown in Figure 1c, the degree of vibrational structure present in the flank toward higher wavelengths above 520 nm is a measure of the extension of the π-conjugated system.[35] It is slightly more pronounced for the P3HT samples. The maximum of the absorption band is shifted to lower wavelength when P3P6T is combined with TiO_2, which indicates interaction of the polymer with nanoparticles (NPs) of positive surface charge.[36] In contrast, P3HT has no negatively charged side groups that could interact with the positively charged NPs.

The crystallite size is obtained via the Scherrer equation from Gaussian fits to the polymer peaks in the XRD spectra (see Figure 1d). With (11.7 ± 0.6) and (11.2 ± 1.0) nm, crystallites are twice as big for P3HT and P3HT:TiO_2, respectively, as compared to P3P6T and P3P6T:TiO_2 ((5.95 ± 0.06) and (6.02 ± 0.16) nm). For both P3HT and P3P6T, the crystalline fraction is considerably reduced in the sample blended with NPs as compared to the neat sample, pointing to a disruption of the interchain order due to the inorganic acceptor particles, as reported before.[37−39]

Optical excitation of the polymer films at 500 nm leads to generation of different polaron species. Their temporal evolution is monitored via the transient response of corresponding IRAVs in the spectral region between 1185 and 1320 cm^{-1}. No degradation of the samples occurs in the course of the measurement for employed pump fluences of <50 $\mu J/cm^2$ (data shown in Figures 2, 3 and Figure S2), as evidenced by subsequent scans at the same sample position that do not show any significant change in amplitude or dynamics for P3HT. The changes observed in P3P6T under the same fluence are attributed to the influence of long-lived photoinduced effects as observed in the FTIR measurements (see Figure S3).

The results measured on P3P6T and P3P6T:TiO_2 are summarized in Figure 2. For better comparison, the transient data shown are normalized to the maximum of the initial absorption at 1218 cm^{-1}. The maximum change in optical density (ΔOD) without normalization lies between 0.5 and 0.8 × 10^{-3}. Two distinct contributions can be identified by their different lifetimes and spectral positions. In pure P3P6T, a short-lived band located below 1260 cm^{-1} is followed by an absorption centered around 1280 cm^{-1} (see Figure 2a). The latter retains its spectral shape for delay times up to 3 ns. The spectrum of the long-lived species averaged from 300 ps to 3 ns matches the PIA as observed in the FTIR spectra (see Figure

DOI: 10.1021/acs.jpcc.9b09820
J. Phys. Chem. C 2019, 123, 28100−28105

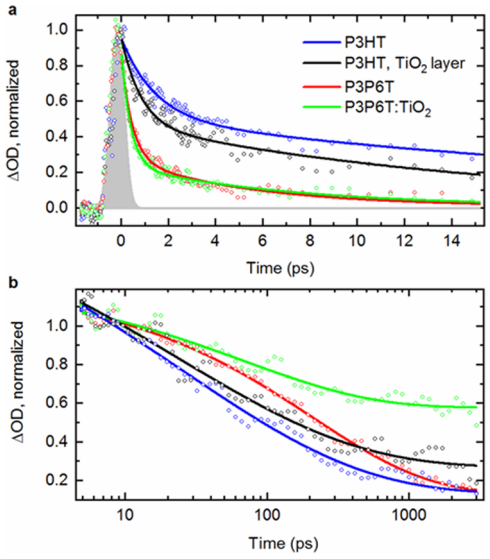

Figure 3. (a) Polaron pair dynamics at 1218 cm^{-1} modeled with a biexponential fit. Contributions from polaron absorption have been subtracted (see text). Indicated in gray is a Gaussian-shaped correlation function, fitted to the rising flank of the signal. (b) Transient dynamics of the polaron band around 1281 cm^{-1} normalized at 10 ps. Stretched exponential fits model polaron diffusion in the polymer.

S4). Therefore, we identify the observed absorption changes as IRAVs due to polarons on the backbone of the polymer, whereas their precursor is assigned to polaron pairs.

When an acceptor in the form of TiO_2 is present, the IR spectral shape is not fundamentally altered compared to neat P3P6T (see Figure 2a,b). However, the amplitude of polarons compared to polaron pairs increases by about 44% (refer to Figures 2c,d), indicating a higher polaron yield from either exciton or polaron pair dissociation. Similar spectral dynamics is observed in P3HT (see Figure S2). The addition of NPs likewise leads to higher amplitude for the polaron signal by about 27%.

Although excitonic signatures in the mid-IR have been suggested on the basis of DFT simulations,[40] we do not observe exciton dynamics in the spectral range investigated. In general, addition of an acceptor leads to more efficient dissociation of excitons at the donor−acceptor interface, reflected in quenching of the exciton signal.[41] Similarly, we would expect a significant reduction of the respective IR absorption signal in P3HT:TiO_2 where efficient charge separation is known to occur. Exciton dissociation within the first 150 fs for P3HT mixed with an inorganic acceptor[42] and even faster in other systems[43,44] has been reported. However, no amplitude reduction of the initial signal is apparent in our measurements. The initial amplitude in the P3HT:TiO_2 sample is 80% of that in the pure polymer despite the more than four times higher absorption of the latter at the spectral position of the pump (see the unscaled UV−vis spectra in Figure S5).

The presence of intrachain polaron pairs was demonstrated before in polyfluorene samples[45,46] where the characterization of the respective polaronic species was based on the intensity dependence of their kinetics. Here, we not only show that they can readily be distinguished, without the need for modeling their respective decay dynamics. Moreover, the general potential of IRAVs as a dynamic indicator of structural disturbances due to the presence of a charge is highlighted.

Whether polaron pairs are generated independently from excitons at the earliest stages or evolve primarily from them is still under debate.[41,47] The formation of polaron pairs has been reported to be as fast as <20 fs in P3HT,[48] well below the time resolution of our experiment. Therefore, this question is not addressed here.

The polaron pair signal at delay times of a few picoseconds is superimposed by the tail of polaron absorption. To separately examine respective contributions, the absorption change related to polarons at 1281 cm^{-1} is scaled to coincide for longer delay times with the signal at 1218 cm^{-1}, where polaron pair absorption is prominent, and subtracted from it. After 200 ps, the dynamics at both spectral positions are identical. The extracted data are presented in Figure 3a. A biexponential fit is modeled to the isolated polaron pair dynamics for each sample. The initial short lifetime of τ_1 = 0.5 ps in P3P6T is followed by a decay with τ_2 = 5.3 ps. Amplitude and time constant only change slightly in the presence of the acceptor (τ_1 = 0.4 ps, τ_2 = 7.1 ps for P3P6T:TiO_2). This suggests that polaron pairs are a bulk effect of the polymer, not impacted largely by the donor/acceptor interface. In comparison, polaron pair decay in the P3HT systems is slower, with τ_1 at around 1 ps (1.4 ps in P3HT and 0.8 ps for P3HT:TiO_2) and a longer second decay constant of 30 ps for the pure polymer and 16 ps in the blend. Since the lifetime and amplitude of the slower decay are somewhat sensitive to the scaling of the subtracted component, not too much weight should be given to their variation. We attribute the sub-ps component in P3P6T to residual bimolecular recombination of polaron pairs that becomes accelerated and more dominant at higher excitation energies. As Figure S6 demonstrates, contributions of such small amplitude do not influence lifetimes measured for the subsequent decay process and thus are not an obstruction to their interpretation.

On timescales longer than a few picoseconds, dynamics is dominated by polaron diffusion[49] either along the backbone of a single polymer strand (intrachain) or in an interchain process from one polymer to another.[47,50] Which process predominates is influenced by the respective degree of intrachain and interchain order within aggregates.[12,51] Intrachain and interchain orders, in turn, are themselves competing characteristics.[52] Diffusion-controlled polaron recombination can be modeled by a stretched exponential decay according to $\Delta\mathrm{OD}(t) \propto \left(\exp\left[-\left(\frac{t}{\tau}\right)^{\beta}\right] + y_0\right)$. In this model, the value of β indicates whether the described motion happens predominantly in one, two, or three dimension.[53,54]

The polaron signal, averaged over the range from 1270 to 1290 cm^{-1}, is presented in Figure 3b for all samples investigated. The data are normalized to the signal at 10 ps and fitted with stretched exponential curves from 5 ps onward. The extracted stretching factor of 0.34 in both P3P6T samples can be attributed to a mostly 1D intrachain motion, as usually associated with β = 1/3. It is paired with similar fast decay times of τ = 23 ps for P3P6T and τ= 26 ps in P3P6T:TiO_2. For P3HT, a more pronounced interchain character is expected. Here, π-stacking is more extended,[55] as evidenced by structuring of UV−vis spectra and the larger crystallite size measured in XRD measurements (see Figure 1). Intrachain effects are still expected to play a role due to the presence of

DOI: 10.1021/acs.jpcc.9b09820
J. Phys. Chem. C 2019, 123, 28100−28105

more ordered macromolecules in P3HT of high molecular weight (>50 kg/mol), as used here.[56] Accordingly, a stretching factor of about 1/2 indicates a mostly two-dimensional diffusion process. Respective timescales are considerably longer than in P3P6T (P3HT: τ = 210 ps, β = 0.53; P3HT:TiO_2: τ = 70 ps, β = 0.48). The share of polarons surviving up to 3 ns is by far the largest for P3HT:TiO_2. For P3P6T, on the other hand, the surviving fraction is reduced to about 17% of its amplitude at 10 ps when TiO_2 is mixed in. It seems to be that the disorder introduced by the acceptor particles in combination with the predominantly one-dimensional nature of the diffusive transport entails a more pronounced recombination of polarons.

CONCLUSIONS

We demonstrate the potential of directly distinguishing polaronic species in conjugated systems via femtosecond mid-IR spectroscopy on infrared-activated vibrations. We have identified polaron pairs with a lifetime on the picosecond scale and polarons decaying over the course of a few hundreds of picoseconds in P3HT and the water-soluble polythiophene derivative P3P6T. This assignment is based on distinct spectral and temporal dynamics and is further supported by the increased ratio of generated polarons in comparison to polaron pairs upon the addition of TiO_2 nanoparticles as an acceptor. The prevalence of contributions due to either intra- or interchain processes in polaron diffusion is in line with the degree of order present in the respective polymer films. However, vibrational modes sensitive to the presence of a charge are not a feature unique to polymers but should instead also give access to polaron dynamics in other emerging photovoltaic materials. Prominent among these are certainly metal halide perovskites where coupling of electronic excitation and molecular vibrations is believed to play a pivotal role.

ASSOCIATED CONTENT

Supporting Information

The Supporting Information is available free of charge on the ACS Publications website at DOI: 10.1021/acs.jpcc.9b09820.

Recovery of FTIR spectrum after illumination, details on time-resolved measurements on P3P6T, pump-probe data for P3HT and P3HT:TiO_2, unscaled UV−vis spectra, and additional FTIR spectra (PDF)

AUTHOR INFORMATION

Corresponding Author

*E-mail: hristo.iglev@ph.tum.de.

ORCID

Klara Stallhofer: 0000-0001-6314-0156
Matthias Nuber: 0000-0002-4409-3590
Volker Körstgens: 0000-0001-7178-5130
Peter Müller-Buschbaum: 0000-0002-9566-6088

Notes

The authors declare no competing financial interest.

ACKNOWLEDGMENTS

We acknowledge the Deutsche Forschungsgemeinschaft (DFG) for the financial support via the Cluster of Excellence "Munich-Centre of Advanced Photonics (MAP)" and the Cluster of Excellence "Nanosystems Initiative Munich (NIM)". We also thank Wolfgang Zinth for infrastructure support and discussions related to femtosecond IR spectroscopy.

REFERENCES

(1) Reid, O. G.; Pensack, R. D.; Song, Y.; Scholes, G. D.; Rumbles, G. Charge Photogeneration in Neat Conjugated Polymers. *Chem. Mater.* **2014**, *26*, 561−575.

(2) Clarke, T. M.; Durrant, J. R. Charge Photogeneration in Organic Solar Cells. *Chem. Rev.* **2010**, *110*, 6736−6767.

(3) Ziemelis, K. E.; Hussain, A. T.; Bradley, D. D. C.; Friend, R. H.; Rühe, J.; Wegner, G. Optical Spectroscopy of Field-Induced Charge in Poly(3-Hexyl Thienylene) Metal-Insulator-Semiconductor Structures: Evidence for Polarons. *Phys. Rev. Lett.* **1991**, *66*, 2231−2234.

(4) Guo, J.; Ohkita, H.; Benten, H.; Ito, S. Near-IR Femtosecond Transient Absorption Spectroscopy of Ultrafast Polaron and Triplet Exciton Formation in Polythiophene Films with Different Regioregularities. *J. Am. Chem. Soc.* **2009**, *131*, 16869−16880.

(5) Donati, G.; Lingerfelt, D. B.; Petrone, A.; Rega, N.; Li, X. "Watching" Polaron Pair Formation from First-Principles Electron-Nuclear Dynamics. *J. Phys. Chem. A* **2016**, *120*, 7255−7261.

(6) Magnanelli, T. J.; Bragg, A. E. Time-Resolved Raman Spectroscopy of Polaron Pair Formation in Poly(3-hexylthiophene) Aggregates. *J. Phys. Chem. Lett.* **2015**, *6*, 438−445.

(7) Moses, D.; Dogariu, A.; Heeger, A. J. Carrier Density and Quantum Efficiency Measurements in Conjugated Polymers: Ultrafast Photoinduced IRAV Absorption. *Thin Solid Films* **2000**, *363*, 68−71.

(8) Cook, S.; Furube, A.; Katoh, R. Analysis of the Excited States of Regioregular Polythiophene P3HT. *Energy Environ. Sci.* **2008**, *1*, 294−299.

(9) Moses, D.; Dogariu, A.; Heeger, A. J. Ultrafast Detection of Charged Photocarriers in Conjugated Polymers. *Phys. Rev. B* **2000**, *61*, 9373−9379.

(10) Ehrenfreund, E.; Vardeny, Z.; Brafman, O.; Horovitz, B. Amplitude and Phase Modes in Trans-Polyacetylene: Resonant Raman Scattering and Induced Infrared Activity. *Phys. Rev. B* **1987**, *36*, 1535−1553.

(11) Anderson, M.; Ramanan, C.; Fontanesi, C.; Frick, A.; Surana, S.; Cheyns, D.; Furno, M.; Keller, T.; Allard, S.; Scherf, U.; Beljonne, D.; D'Avino, G.; von Hauff, E.; Da Como, E. Displacement of Polarons by Vibrational Modes in Doped Conjugated Polymers. *Phys. Rev. Mater.* **2017**, *1*, 055604.

(12) Ghosh, R.; Chew, A. R.; Onorato, J.; Pakhnyuk, V.; Luscombe, C. K.; Salleo, A.; Spano, F. C. Spectral Signatures and Spatial Coherence of Bound and Unbound Polarons in P3HT Films: Theory Versus Experiment. *J. Phys. Chem. C* **2018**, *122*, 18048−18060.

(13) Zhang, S.; Ye, L.; Zhang, H.; Hou, J. Green-Solvent-Processable Organic Solar Cells. *Mater. Today* **2016**, *19*, 533−543.

(14) Körstgens, V.; Pröller, S.; Buchmann, T.; Moseguí González, D.; Song, L.; Yao, Y.; Wang, W.; Werhahn, J.; Santoro, G.; Roth, S. V.; Iglev, H.; Kienberger, R.; Müller-Buschbaum, P. Laser-Ablated Titania Nanoparticles for Aqueous Processed Hybrid Solar Cells. *Nanoscale* **2015**, *7*, 2900−2904.

(15) Yan, F.; Li, J.; Mok, S. M. Highly Photosensitive Thin Film Transistors Based on a Composite of Poly(3-Hexylthiophene) and Titania Nanoparticles. *J. Appl. Phys.* **2009**, *106*, 074501.

(16) Sun, Z.; Li, J.; Liu, C.; Yang, S.; Yan, F. Enhancement of Hole Mobility of Poly(3-Hexylthiophene) Induced by Titania Nanorods in Composite Films. *Adv. Mater.* **2011**, *23*, 3648−3652.

(17) Song, L.; Abdelsamie, A.; Schaffer, C. J.; Körstgens, V.; Wang, W.; Wang, T.; Indari, E. D.; Fröschl, T.; Hüsing, N.; Haeberle, T.; Lugli, P.; Bernstorff, S.; Müller-Buschbaum, P. A Low Temperature Route Toward Hierarchically Structured Titania Films for Thin Hybrid Solar Cells. *Adv. Funct. Mater.* **2016**, *26*, 7084−7093.

(18) Grupp, A.; Ehrenreich, P.; Kalb, J.; Budweg, A.; Schmidt-Mende, L.; Brida, D. Incoherent Pathways of Charge Separation in Organic and Hybrid Solar Cells. *J. Phys. Chem. Lett.* **2017**, *8*, 4858−4864.

(19) Tulsiram, N.; Kerr, C.; Chen, J. I. L. Photoinduced Charge Transfer in Poly(3-hexylthiophene)/TiO_2 Hybrid Inverse Opals:

DOI: 10.1021/acs.jpcc.9b09820
J. Phys. Chem. C 2019, 123, 28100−28105

Photonic vs Interfacial Effects. *J. Phys. Chem. C* **2017**, *121*, 26987−26996.
(20) Chen, T.-A.; Wu, X.; Rieke, R. D. Regiocontrolled Synthesis of Poly(3-alkylthiophenes) Mediated by Rieke Zinc: Their Characterization and Solid-State Properties. *J. Am. Chem. Soc.* **1995**, *117*, 233−244.
(21) Gasgnier, M. IR Spectra of Some Potassium Carboxylates. *J. Mater. Sci. Lett.* **2001**, *20*, 1259−1262.
(22) Stimson, M. M. Sodium and Potassium Cation Dependence of the Infrared Absorption of COO^-. *J. Chem. Phys.* **1954**, *22*, 1942.
(23) Lane, P. A.; Wei, X.; Vardeny, Z. V. Studies of Charged Excitations in π-Conjugated Oligomers and Polymers by Optical Modulation. *Phys. Rev. Lett.* **1996**, *77*, 1544−1547.
(24) Österbacka, R.; Jiang, X. M.; An, C. P.; Horovitz, B.; Vardeny, Z. V. Photoinduced Quantum Interference Antiresonances in π-Conjugated Polymers. *Phys. Rev. Lett.* **2002**, *88*, 226401.
(25) Jiang, X. M.; Österbacka, R.; Korovyanko, O.; An, C. P.; Horovitz, B.; Janssen, R. A. J.; Vardeny, Z. V. Spectroscopic Studies of Photoexcitations in Regioregular and Regiorandom Polythiophene Films. *Adv. Funct. Mater.* **2002**, *12*, 587−597.
(26) Kahmann, S.; Loi, M. A.; Brabec, C. J. Delocalisation Softens Polaron Electronic Transitions and Vibrational Modes in Conjugated Polymers. *J. Mater. Chem. C* **2018**, *6*, 6008−6013.
(27) Li, H.; Zhang, Y.; Zhang, S.-L.; Qiu, Z.-J. Trion-Induced Current Anomaly in Organic Polymer. *Org. Electron.* **2016**, *34*, 124−129.
(28) Drori, T.; Gershman, E.; Sheng, C. X.; Eichen, Y.; Vardeny, Z. V.; Ehrenfreund, E. Illumination-induced Metastable Polaron-supporting State in Poly(*p*-Phenylene Vinylene) Films. *Phys. Rev. B* **2007**, *76*, 033203.
(29) Chwang, A. B.; Frisbie, C. D. Temperature and Gate Voltage Dependent Transport Across a Single Organic Semiconductor Grain Boundary. *J. Appl. Phys.* **2001**, *90*, 1342−1349.
(30) Kaake, L. G.; Barbara, P. F.; Zhu, X.-Y. Intrinsic Charge Trapping in Organic and Polymeric Semiconductors: A Physical Chemistry Perspective. *J. Phys. Chem. Lett.* **2010**, *1*, 628−635.
(31) Horowitz, G.; Hajlaoui, M. E.; Hajlaoui, R. Temperature and Gate Voltage Dependence of Hole Mobility in Polycrystalline Oligothiophene Thin Film Transistors. *J. Appl. Phys.* **2000**, *87*, 4456−4463.
(32) Schön, J. H.; Kloc, C. Charge Transport Through a Single Tetracene Grain Boundary. *Appl. Phys. Lett.* **2001**, *78*, 3821−3823.
(33) Neto, N. M. B.; Silva, M. D. R.; Araujo, P. T.; Sampaio, R. N. Photoinduced Self-Assembled Nanostructures and Permanent Polaron Formation in Regioregular Poly(3-hexylthiophene). *Adv. Mater.* **2018**, *30*, 1705052.
(34) Klöpffer, W. *Introduction to Polymer Spectroscopy*; Springer: Berlin, Heidelberg, 1984.
(35) Marsh, R. A.; Hodgkiss, J. M.; Albert-Seifried, S.; Friend, R. H. Effect of Annealing on P3HT:PCBM Charge Transfer and Nanoscale Morphology Probed by Ultrafast Spectroscopy. *Nano Lett.* **2010**, *10*, 923−930.
(36) Suttiponparnit, K.; Jiang, J.; Sahu, M.; Suvachittanont, S.; Charinpanitkul, T.; Biswas, P. Role of Surface Area, Primary Particle Size, and Crystal Phase on Titanium Dioxide Nanoparticle Dispersion Properties. *Nanoscale Res. Lett.* **2011**, *6*, 27.
(37) Lilliu, S.; Agostinelli, T.; Pires, E.; Hampton, M.; Nelson, J.; Macdonald, J. E. Dynamics of Crystallization and Disorder During Annealing of P3HT/PCBM Bulk Heterojunctions. *Macromolecules* **2011**, *44*, 2725−2734.
(38) Agostinelli, T.; Lilliu, S.; Labram, J. G.; Campoy-Quiles, M.; Hampton, M.; Pires, E.; Rawle, J.; Bikondoa, O.; Bradley, D. D. C.; Anthopoulos, T. D.; Nelson, J.; Macdonald, J. E. Real-Time Investigation of Crystallization and Phase-Segregation Dynamics in P3HT:PCBM Solar Cells During Thermal Annealing. *Adv. Funct. Mater.* **2011**, *21*, 1701−1708.
(39) Collins, B. A.; Tumbleston, J. R.; Ade, H. Miscibility, Crystallinity, and Phase Development in P3HT/PCBM Solar Cells: Toward an Enlightened Understanding of Device Morphology and Stability. *J. Phys. Chem. Lett.* **2011**, *2*, 3135−3145.
(40) Yin, J.; Wang, Z.; Fazzi, D.; Shen, Z.; Soci, C. First-Principles Study of the Nuclear Dynamics of Doped Conjugated Polymers. *J. Phys. Chem. C* **2016**, *120*, 1994−2001.
(41) Miranda, P. B.; Moses, D.; Heeger, A. J. Ultrafast Photogeneration of Charged Polarons in Conjugated Polymers. *Phys. Rev. B* **2001**, *64*, 081201.
(42) Herrmann, D.; Niesar, S.; Scharsich, C.; Köhler, A.; Stutzmann, M.; Riedle, E. Role of Structural Order and Excess Energy on Ultrafast Free Charge Generation in Hybrid Polythiophene/Si Photovoltaics Probed in Real Time by Near-Infrared Broadband Transient Absorption. *J. Am. Chem. Soc.* **2011**, *133*, 18220−18233.
(43) Grancini, G.; Maiuri, M.; Fazzi, D.; Petrozza, A.; Egelhaaf, H.-J.; Brida, D.; Cerullo, G.; Lanzani, G. Hot Exciton Dissociation in Polymer Solar Cells. *Nat. Mater.* **2013**, *12*, 29−33.
(44) Hwang, I.-W.; Moses, D.; Heeger, A. J. Photoinduced Carrier Generation in P3HT/PCBM Bulk Heterojunction Materials. *J. Phys. Chem. C* **2008**, *112*, 4350−4354.
(45) Virgili, T.; Marinotto, D.; Manzoni, C.; Cerullo, G.; Lanzani, G. Ultrafast Intrachain Photoexcitation of Polymeric Semiconductors. *Phys. Rev. Lett.* **2005**, *94*, 117402.
(46) Westerling, M.; Aarnio, H.; Österbacka, R.; Stubb, H.; King, S. M.; Monkman, A. P.; Andersson, M. R.; Jespersen, K.; Kesti, T.; Yartsev, A.; Sundström, V. Photoexcitation Dynamics in an Alternating Polyfluorene Copolymer. *Phys. Rev. B* **2007**, *75*, 224306.
(47) Korovyanko, O. J.; Österbacka, R.; Jiang, X. M.; Vardeny, Z. V.; Janssen, R. A. J. Photoexcitation Dynamics in Regioregular and Regiorandom Polythiophene Films. *Phys. Rev. B* **2001**, *64*, 235122.
(48) de Sio, A.; Troiani, F.; Maiuri, M.; Réhault, J.; Sommer, E.; Lim, J.; Huelga, S. F.; Plenio, M. B.; Rozzi, C. A.; Cerullo, G.; Molinari, E.; Lienau, C. Tracking the Coherent Generation of Polaron Pairs in Conjugated Polymers. *Nat. Commun.* **2016**, *7*, 13742.
(49) Kanner, G. S.; Wei, X.; Hess, B. C.; Chen, L. R.; Vardeny, Z. V. Evolution of Excitons and Polarons in Polythiophene from Femtoseconds to Milliseconds. *Phys. Rev. Lett.* **1992**, *69*, 538−541.
(50) Markov, D. E.; Blom, P. W. M. Anisotropy of Exciton Migration in Poly(p-Phenylene Vinylene). *Phys. Rev. B* **2006**, *74*, 085206.
(51) Scholes, D. T.; Yee, P. Y.; Lindemuth, J. R.; Kang, H.; Onorato, J.; Ghosh, R.; Luscombe, C. K.; Spano, F. C.; Tolbert, S. H.; Schwartz, B. J. The Effects of Crystallinity on Charge Transport and the Structure of Sequentially Processed F_4TCNQ-Doped Conjugated Polymer Films. *Adv. Funct. Mater.* **2017**, *27*, 1702654.
(52) Spano, F. C.; Silva, C. H- and J-aggregate Behavior in Polymeric Semiconductors. *Annu. Rev. Phys. Chem.* **2014**, *65*, 477−500.
(53) Yan, M.; Rothberg, L. J.; Papadimitrakopoulos, F.; Galvin, M. E.; Miller, T. M. Defect Quenching of Conjugated Polymer Luminescence. *Phys. Rev. Lett.* **1994**, *73*, 744−747.
(54) Koyama, T.; Nakamura, A.; Kishida, H. Microscopic Mobility of Polarons in Chemically Doped Polythiophenes Measured by Employing Photoluminescence Spectroscopy. *ACS Photonics* **2014**, *1*, 655−661.
(55) Sirringhaus, H.; Brown, P. J.; Friend, R. H.; Nielsen, M. M.; Bechgaard, K.; Langeveld-Voss, B. M. W.; Spiering, A. J. H.; Janssen, R. A. J.; Meijer, E. W.; Herwig, P.; de Leeuw, D. M. Two-Dimensional Charge Transport in Self-Organized, High-Mobility Conjugated Polymers. *Nature* **1999**, *401*, 685−688.
(56) Paquin, F.; Yamagata, H.; Hestand, N. J.; Sakowicz, M.; Bérubé, N.; Côté, M.; Reynolds, L. X.; Haque, S. A.; Stingelin, N.; Spano, F. C.; Silva, C. Two-dimensional Spatial Coherence of Excitons in Semicrystalline Polymeric Semiconductors: Effect of Molecular Weight. *Phys. Rev. B* **2013**, *88*, 155202.

DOI: 10.1021/acs.jpcc.9b09820
J. Phys. Chem. C 2019, 123, 28100−28105